Experimental Simulation of the Human Respiration

Andreas Kohl, Pascal Lange(✉), and Daniel Schmeling

German Aerospace Center (DLR), Institute of Aerodynamics and Flow Technologies, Bunsenstraße 10, 37073 Göttingen, Germany
{andreas.kohl,pascal.lange,daniel.schmeling}@dlr.de

Abstract. In this paper, we present a new mobile respiration simulation system (RSS), which can be connected to existing thermal manikins. With the objective to simulate the human respiration process as realistic as possible, the system was validated on the basis of literature data and results obtained from human subject tests. The RSS reproduces realistic respiration cycles characterized by a sine wave of a typical normal breathing flow rate. The provided flow rates as well as the breathing frequency – representing the time of inhalation and exhalation – were verified by literature values. Since the new system additionally allows to enrich the exhaled air with carbon dioxide (CO_2), experimental studies addressing the indoor air quality are also feasible. Here, the amount of CO_2 emitted by the RSS corresponds to the average amount of CO_2 exhaled by test persons. In addition, the flow characteristics occurring in a human nose are simulated using a self-developed facial mask, in combination with the new system. The result is a breathing thermal manikin based on a mobile respiration simulation system, which can easily be connected to heated passenger models. Accordingly, the system can be installed at any seat within a passenger compartment. This offers the advantage of individually defining the location of the manikin, which can effortlessly be adapted during a measurement campaign. Therefore, the system especially suitable for studies addressing the performance of ventilation systems in passenger compartments and indoor environments.

Keywords: Indoor air quality · Breathing thermal manikin · CO_2 distribution · Passenger comfort · Ventilation efficiency · Airborne spreading

1 Introduction

For many decades, thermal manikins (TMs) have been widely used in research activities addressing the thermal passenger comfort in cabins, such as trains or airplanes, as well as for experimental studies regarding the airflow in indoor environments, e.g. in office buildings [1]. The manikins simulate the geometrical blockage and the sensible heat release of humans. TMs provide repeatable and comparable experimental setups with well-known and precise boundary conditions required for the implementation in computational fluid dynamics (CFD)

A. Dillmann et al. (Eds.): STAB/DGLR Symposium 2020, NNFM 151, pp. 472–482, 2021.
https://doi.org/10.1007/978-3-030-79561-0_45

simulations. Additionally, so-called "breathing thermal manikins" (BTM) are used to simulate the human respiration, i.e. the forced convective airflow caused by in- and exhalation. The combination of the room ventilation, the thermal convection induced by the human heat release and the forced respiration flow determine the airflow around the human body [2]. The present report describes the development and testing of a human respiration simulation system (RSS), which can be attached to existing TMs currently used at the DLR in Göttingen. In addition to the simulation of the airflow through inhalation and exhalation, the system can also emit the same amount of the respiration waste gas CO_2 as a real human would do. Here, CO_2 is an important indicator for the indoor air quality affecting comfort, health and productivity of the passengers [3]. Modern passenger trains take this issue into account by adjusting the volume flow rate of the fresh air based on interior CO_2 concentrations.

The rapidly developing situation of the corona pandemic in 2020 also leads to the fact that studies regarding air quality, air pollution level and airborne transmission of infectious agents become more and more relevant. Recent studies have proven that tracer gas is a suitable surrogate for exhaled aerosols (smallest liquid droplets) [4]. For this reason, during tracer gas measurements the RSS can be used as a source to dose gas while simulating the respiration process. Consequently, the study of these transport processes forms the basis for developing new ventilation scenarios, focusing on a high contaminant removal efficiency.

In the following sections, the developed RSS is introduced and first test measurements are presented in order to validate the new system. The latter comprise measurements to analyze the performance of the system with regard to typical human breathing profiles and CO_2 exhalation rates. In a second step, the latest results of the application of the RSS in a generic train laboratory are shown.

2 Human Breathing Characteristics

This chapter includes the description of the basic parameters and characteristics of the human respiration process given in the literature. The newly developed RSS is based on the findings regarding the respiration cycle of a human as well as on the breathing flow caused by human respiration. The mechanical parts, the electrics as well as the measurement and control system have been designed to simulate the human respiration process as realistically as possible.

The human respiration process is driven by the lifting and lowering of the chest and the diaphragm resulting in a compression and decompression of the lungs. Therefore, the air inside the lungs is exchanged with the environmental air through the nose and mouth. Inside the lungs, oxygen (O_2) contained in the inhaled air is exchanged with CO_2 in the blood which is produced during cellular respiration in the human metabolism. The average breathing frequency (BF) of humans is between 10 and 15 breaths per minute for normal tidal breathing without physical exertion [5]. The volume that is exchanged during tidal breathing corresponds to the tidal volume of about 0,6 l. These values of the volume and BF are implemented as standard breathing setting of the RSS. Further, during normal breathing, a human emits between 250 and 300 ml of CO_2 per minute [5]

which corresponds to about 4% of the tidal volume. The RSS also facilitates the provision of the mentioned CO_2 quantities. Moreover, breathing during physical or mental exertion can also be simulated by the RSS by modifying the settings (e.g. raise of BF, tidal volume and emitted CO_2 quantity).

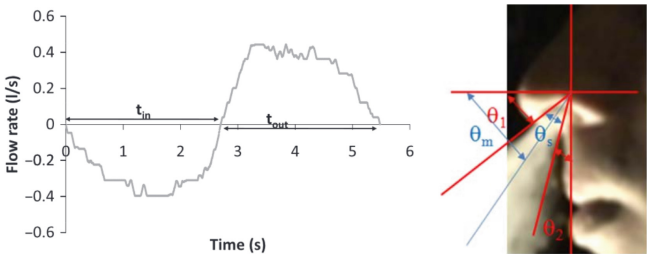

Fig. 1. Flow rate of humans during tidal breathing [6] (left). Side view of the visualized exhalation jets through the nose [6] (right).

The work of Gupta *et al.* [6] analyzes the breathing flow rate of 25 test persons. The typical volume flow of the respiration process is sinusoidal as shown in Fig. 1 (left) and reaches peak flow rates of around ± 0.4 l/s for an average human and may vary depending on the physiological state of the individual person [6]. In addition to the simulation of the tidal breathing, the system is designed to measure the generated flow rate and to analyze the inhaled air in terms of CO_2 level, temperature and humidity.

Figure 1 (right) shows the human airflow caused by exhalation through the nose according to [6]. The findings regarding the mean flow angles of spreading (Θ_s) and from the side (Θ_m) are given in Eq. (1).

$$\Theta_s = 23° \pm 14° \quad \Theta_m = 60° \pm 6° \tag{1}$$

Moreover, an average nose opening for male subjects during breathing was determined in [6] and amounts to $0,71 \pm 0,23\,\mathrm{cm}^2$. These criteria serve as a guideline for designing a male face mask, which can be connected to the RSS in order to reproduce the corresponding flow angles through the nose.

3 System Layout and Implementation

3.1 Mechanical Implementation

The mechanical implementation is shown as a technical principle in Fig. 2 on the left. The stepper motor is connected via clutch to a spindle, which rotates in both directions. The stepper motor operates in closed-loop control for better acceleration and to avoid step loss as well as resonance frequencies. The rotation is translated into a linear movement by a screw nut and a linear stage. This linear movement y compresses and decompresses the two bellow cylinders, which simulate the human lungs and provide the breathing volume flow $\dot{V}$. In one bellow cylinder the inhaled air is analyzed and in the second cylinder CO_2 is dosed by a solenoid valve (see Fig. 2, right). Detailed information regarding the system components and the design process are given in [7].

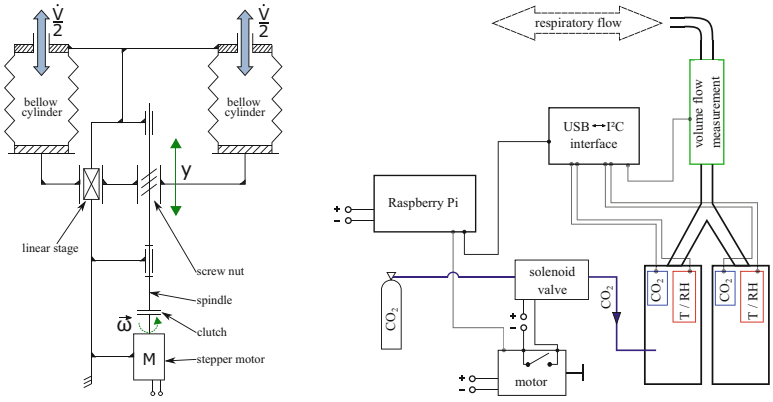

Fig. 2. Technical principle of the RSS [7] (left). Sketch of the control system including the sensor positions, represented by green, blue and red rectangles (right).

3.2 Sensors and Control System

The control system is based on a small single board computer ("Raspberry Pi"), which is responsible for controlling the sensors and sending trigger signals to the motor (see Fig. 2, right). The used sensors comprise a bidirectional volume flow sensor (accuracy: ±1.5%), several CO_2 detectors (accuracy: ±30 ppm + 3%) as well as temperature (accuracy: ±0.1 °C) and humidity probes (accuracy: ±1.5%). The motor features its own system to ensure the closed-loop control in order to control the movement as well as the opening of the solenoid valve, as indicated in Fig. 2, right. The amount of CO_2 emitted in the system depends on the opening time of the valve (τ_V) and is precisely adjustable in steps of 0,1 ml (corresponds to an opening time of 1 ms). The CO_2 is stored in a pressure bottle connected to the system via tubing under a predefined pressure. For detailed information regarding the electrical setup of the RSS see [7].

3.3 Development of a Realistic Human Breathing Flow via Facial Mask

As shown in Fig. 3 (left), the face mask was constructed using a three-dimensional scan of a male face [8] and manufactured using a 3D printing process. The mask is connectable to the RSS using standardized hose parts. Subsequently, the mask is attached to the manikin's face. So far only the respiration through the nose has been simulated. However, a mask supporting breathing through the mouth has recently been developed. The resulting exhalation flow angles are depicted in Fig. 3 (right) and will be discussed in the following section.

4 System Validation and Application

4.1 Validation of Human Breathing Characteristics

Before the RSS can be used for experimental simulation of the human breathing process, both the volume flow characteristics and the amount of exhausted CO_2

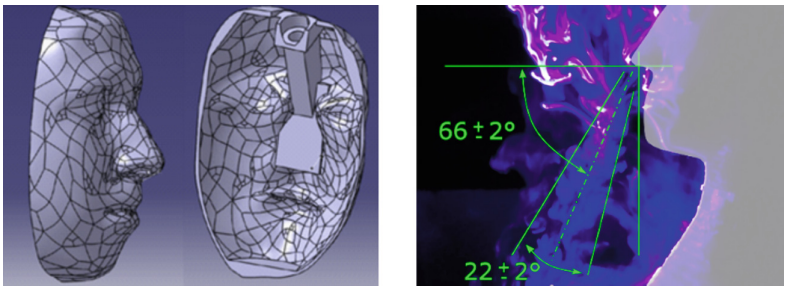

Fig. 3. 3D model of a human facial mask (left). Analysis of the resulting flow pattern through the facial mask (right).

must be calibrated based on the real human metabolism. These characteristics are adjusted by controlling the motor control curve and the opening time of the magnetic valve, respectively. In a first step, the volume flow rate provided by the RSS is compared to the data given in [6], see Fig. 4 (left). For a system's BF of 11 min^{-1} (represented by red triangles), the flow rate of a breathing cycle matches the literature data [6] (grey circles) with the following mean deviations of 1.5% for the tidal volume, 0.5% for the peak values and 0.4% for the frequency.

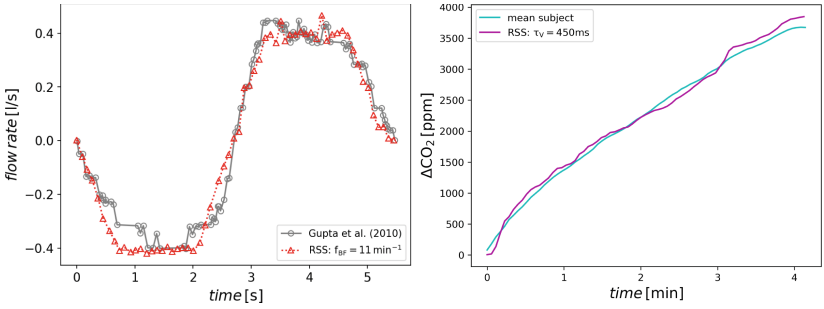

Fig. 4. Validation tests of provided breathing flow rate (left). Results of the validation regarding emitted CO_2 amount (right).

In a second step, the emitted amount of CO_2 is validated by measurements with test persons. For this purpose, the subjects breathed into an enclosed environment (volume $\approx 230\,\text{l}$) over a period of four minutes. The resulting enrichment of CO_2 (cyan colored line), up to a maximum value of 3675 ppm, is shown in Fig. 4 (right) and serves as a benchmark for the RSS. By modifying the opening time of the solenoid valve (see Fig. 2, right), the emitted amount of CO_2 provided by the system can be varied. As shown in Fig. 4 (right), an opening time of $\tau_V = 450\,\text{ms}$ (magenta colored line) results in a CO_2 exhaust rate, which matches the mean subject values with a mean accuracy of 1.8%. The last step comprises the validation of the flow characteristics through the human facial

mask. In order to do so, a flow visualization with laser light and smoke is conducted. The resulting flow pattern including the flow angles provided by the generic facial mask is analyzed using a graphical editing software. As illustrated in Fig. 3 (right), the determined angles agree with the values given in Eq. (1) within measurement accuracy. In conclusion, it should be noted, that the human breathing process is highly individual and furthermore strongly depend on the level of activity. For the calibration of the RSS we used mean values from the literature, hence, the RSS represents a "standardized average human".

4.2 Generic Train Laboratory

The application tests are carried out in a generic train laboratory, a full-scale mock-up with the realistic geometry of the DLR's next generation train (NGT), see Fig. 5 (left). The lower deck is suitable for experimental studies addressing air conditioning, thermal passenger comfort, energy efficiency and indoor air quality. The mock-up is equipped with 24 real train seats from a regional train (see Fig. 5, right), which are separated in six seat rows. TMs are used to simulate the sensible heat impact and the obstruction of passengers.

Fig. 5. CAD model of the generic train laboratory [9] (left). Cabin partly equipped with TMs and with installed hatrack-integrated air supply inlets (right).

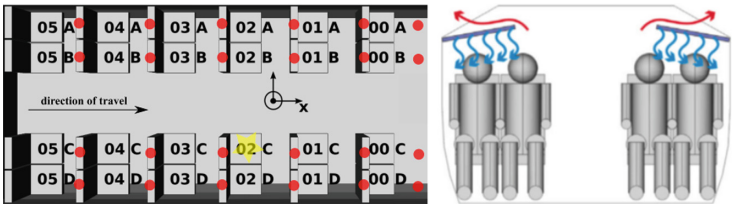

Fig. 6. Seating plan with CO_2 sensor positions (red dots) and CO_2 source location (yellow star), (left). Illustration of HLMV [10] (right).

A comprehensive sensor system comprising local temperature, humidity and CO_2 probes is installed. As indicated in Fig. 6 (left), the respective CO_2 sensors

are attached to the backrest of the seats. The generic train cabin in combination with an air conditioning system facilitates experimental studies of different ventilation scenarios. As shown in Fig. 5 (right), a novel ventilation concept, called hatrack-integrated low-momentum ventilation (HLMV), was installed during the presented studies. It is characterized by a low-momentum air supply above the passenger heads through planar, large-surface outlets, which are integrated in the lower part of the overhead luggage racks (see Fig. 6, right) [10]. After circulation, the air leaves the compartment through slit-shape outlets in the lateral parts of the ceiling.

4.3 Spatial CO_2 Distribution in the Generic Train Laboratory

As a sample application, studies with the RSS are compared to investigations using a human subject as a CO_2 source in a generic train cabin. In both cases, the source is placed on seat position 02C (see, Fig. 6, left). During the tests, the ventilation scenario described in Sect. 4.2 is installed. The temperature of the inflowing air is set to 17.5 °C and maintained with a maximum deviation of less than 2%. The total volume flow rate amounts to 225 ± 5 l/s, which is about twice the amount of fresh air for 24 passengers in accordance with EN13129 [11]. As long-distance trains are typically operated with a recirc fraction of 50%, the volume flow rate in the generic mock-up is similar to the total volume flow rate in real train compartments. During the investigations, the passengers are simulated using TMs, each operating at a constant heat release of 75 W.

Novel Breathing Thermal Manikin as CO_2 Source: For the application test with the new RSS, the latter is connected to a facial mask positioned on a TM's face (see Fig. 7, left).

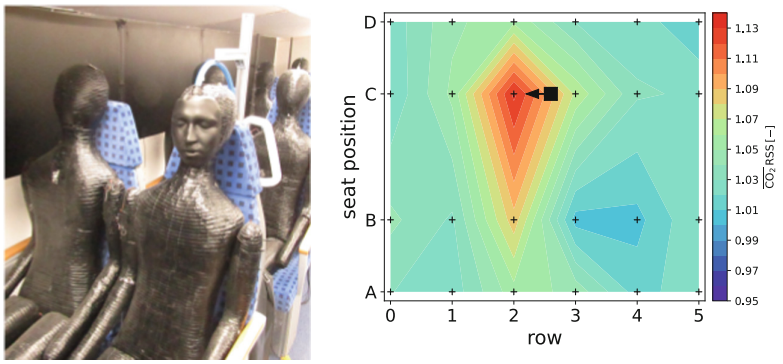

Fig. 7. RSS as a CO_2 source connected to a facial mask at the TM's face (left). Resulting CO_2 distribution within the generic train laboratory caused by the system (right).

After thermal conditions within the cabin have reached a state of equilibrium, the RSS is operated for 45 min. The parameters of the RSS (i.e. BF and

opening time of the valve) are set as described in Sect. 4.1. The resulting CO_2 distribution – averaged over the last 25 min of emission – is shown in Fig. 7 (right). Here, the data is normalized using the mean background concentration of 444 ppm. The black square symbolizes the position of the CO_2 source, while the arrow represents the breathing direction. The supporting measurement positions are marked as black crosses. The resulting distribution shows a significant CO_2 accumulation in the immediate vicinity of the source. The maximum values of 1.13 are found at position 02C. The propagation of the gas is limited to the row in which the source is located, since increased values occur for position 02B, 02C and 02D. The concentration at the seats in front and behind the source increases only slightly. The values at the remaining seat positions are about 1.0 corresponding to background concentration.

Human Subject as CO_2 Source: Subsequently, a human subject is used as CO_2 source. After steady-state conditions are achieved in the lab, the test person sits at position 02C (see Fig. 8, left) for 45 min. The subject was instructed to sit as still as possible and breathe calmly during the test phase. The concentration distribution – averaged over the last 25 min of breathing – is normalized with the background concentration of 460 ppm and depicted in Fig. 8 (right). The black square and the corresponding arrow represent the exact position of the source and the direction of breathing, respectively. The black crosses illustrate the location of the sensors. A maximum normalized concentration of 1.1 occurred at position 02C. Generally higher values are measured for the adjoining seats, such as 03C and 03D. This means that the source clearly induces a significant concentration increase at the adjacent seats behind the source. Considering the seat rows two and three, the released CO_2 remains localized in the area of the lab near the source (seat position C and D) since no noticeable rise in concentration occurred at seat positions 02B/01B and 02A/01A. In this case, values of about 1.0 (representing background concentration) are determined at the remaining seat positions.

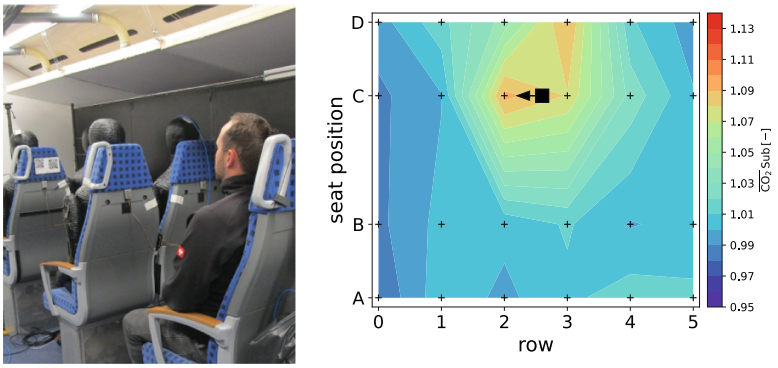

Fig. 8. Human subject as a CO_2 source at seat 02C (left). Resulting CO_2 distribution within the generic train laboratory caused by the test person (right).

Comparison of Mechanical and Human CO_2 Source: To compare the two different sources, the resulting CO_2 distributions in the generic train cabin are taken into account. In both cases, the maximum concentration values occurs directly in front of the source, at seat position 02C. Considering the concentration already existing in the air (background concentration), both types of sources cause the same mean concentration increase (at least for this particular seat position). Therefore, the adjustments to the respiration system, based on the validation tests (see Sect. 4.1), seem to be appropriate to simulate the human breathing characteristics. However, the resulting CO_2 propagation in the cabin shows significant differences for the two investigated sources. Using the RSS as a CO_2 source results in a localized dispersion near the source. Mainly, the emitted gas disseminates in the seat row, where the source is located. Using a human as a CO_2 source also leads to a localized increase in concentration, however, in this case, the source clearly induces accumulations in the adjacent seats, right behind the source location. Further, the gas accumulation seems to remain on the side of the cabin, where the source is located (seat position C and D). In contrast, a propagation in the seat row across the aisle (to position A and B) cannot be observed. A reason for the differences in the results of both investigations could be differently developed flow patterns in the vicinity of the source. The body surface of the TM is smaller compared to a male human. Thus, the TM might emit a lower heat flux density than the test person. Further, the human subject was wearing a jacket, which represents a thermal insulation for the heat release. These facts influence the buoyancy-driven flows and consequently result in differences for the developed flow structures near the source. Furthermore, when using a test person as a CO_2 source, even slight changes of the seating position or small changes of the discharge direction (due to movements of the head) also affect the resulting concentration distribution within the compartment.

5 Conclusion

We introduced a new respiration simulation system, designed and set up at the German Aerospace Center in Göttingen. The system is attachable to a heat-releasing thermal manikin in order to simulate a breathing passenger, especially for research activities addressing the air quality in passenger compartments or indoor environments. To simulate a realistic breathing process, the breathing flow rate was analyzed and compared with literature data, which are based on results of human subject tests. A system's breathing frequency of $11\,\mathrm{min}^{-1}$ leads to a similar respiration curve with a mean deviation of 1.5% and 0.5% for the tidal volume and peak values, respectively. The system also facilitates the dosage of respiration gases, in particular CO_2, similar to the emissions of real persons. Hereto, validation tests with human subjects were conducted to provide realistic CO_2 quantities. The system provide the same CO_2 exhaust rate with a mean deviation of less than 2%. Furthermore, since the gas emission as well as the breathing flow rate of the system are variable, the simulation of different breathing cycles (i.e. during physical exertion) is feasible. Moreover, connecting

a facial mask to the respiration system simulates realistic outflow characteristics through the nose.

In a second step, the performance of the respiration simulation system was verified in a generic train cabin for an alternative ventilation system – hatrack-integrated low-momentum ventilation. Additionally, investigations with a human subject as a CO_2 source were conducted. The resulting spatial CO_2 distribution reveal similar concentration peaks directly in front of the source. However, the distribution paths of the gas are slightly different. While the CO_2 provided by the system remains localized in the seat row where the source is located, the test person induces a concentration increase for the adjacent seats behind the source. The differences in the gas propagation are not only attributed to the system's settings but rather to the different body shape and heat emission of the thermal manikin in contrast to the human subject. Furthermore, the discharge direction during exhalation affects the resulting propagation of CO_2 in the passenger compartment. The human subjects influence the discharge direction due to minor changes in sitting posture and head movements, whereas the breathing thermal manikin sits perfectly still. In spite of these explained smaller deviations in the near field, the new respiration simulation system was successfully taken into operation. The validation tests confirmed the realistic breathing frequency, tidal volume, amplitude values and CO_2 enrichment of the system compared to real humans.

Acknowledgement. The authors acknowledge Annika Köhne for proofreading this manuscript.

References

1. Holmer, I.: Thermal manikin history and applications. Eur. J. Appl. Physiol. **92**(6), 614–618 (2004)
2. Ivanov, M., Mijorski, S.: CFD modelling of flow interaction in the breathing zone of a virtual thermal manikin. Energy Procedia **112**, 240–251 (2017)
3. Dorgan, B., Dorgan, E., Kanarek, M., Willman, A.: Healthy and productivity benefits of improved indoor air quality. ASHRAE Trans. **104**, 658 (1998)
4. Ai, Z., Mak, C., Gao, N., Niu, J.: Tracer gas is a suitable surrogate of exhaled droplet nuclei for studying airborne transmission in the built environment. Build. Simul. **13**, 489–496 (2020)
5. Oczenski, W., Andel, H., Werba, A.: Atmen, Atemhilfen: Atemphysiologie und Beatmungstechnik, 9th edn. Georg Thieme Verlag, Stuttgart (2012)
6. Gupta, J., Lin, C.-H., Chen, Q.: Characterizing exhaled airflow from breathing and talking. Indoor Air **20**(1), 31–39 (2010)
7. Kohl, A.: Entwicklung eines Systems zur experimentellen Simulation der Atmung von Passagieren. Master-thesis, TU Ilmenau (2020)
8. GrabCAD Homepage. http://grabcad.com/library/male-face. Accessed 18 June 2020
9. Schmeling, D., Bosbach, J.: On the influence of sensible heat release on displacement ventilation in a train compartment. Build. Environ. **125**, 248–260 (2017)

10. Schmeling, D., Volkmann, A.: On the experimental investigation of novel low-momentum ventilation concepts for cooling operation in a train compartment. Build. Environ. **182**, 107116 (2020)
11. EN 13129: Railways Application - Air conditioning for mainline rolling stock - Comfort parameters and type tests. German Version EN13129:2016 (2020)